Cooperative mmWave PHD-SLAM with Moving Scatterers

Citation for the original published paper (version of record):
Kim, H., Lee, J., Ge, Y. et al (2022). Cooperative mmWave PHD-SLAM with Moving Scatterers. 2022 25th International Conference on Information Fusion, FUSION 2022. http://dx.doi.org/10.23919/FUSION49751.2022.9841389

Cooperative mmWave PHD-SLAM with Moving Scatterers

Hyowon Kim*, Jaebok Lee†, Yu Ge*, Fan Jiang*, Sunwoo Kim†, and Henk Wymeersch*
* Department of Electrical Engineering, Chalmers University of Technology, Sweden
† Department of Electronic Engineering, Hanyang University, Seoul, Korea

***Abstract*—Simultaneous localization and mapping (SLAM) using multipath at mmWave frequencies can provide accurate localization in the presence of static landmarks. When radio signals reflected from moving vehicle scatterers (VSs) are observed, the standard SLAM filters exhibit a degraded performance. To address this problem, we propose a probability hypothesis density (PHD)-based SLAM filter, where separate maps are maintained for VS and other types of landmarks. Through a combination of developed (i) local PHD-SLAM and (ii) global map fusion, we demonstrate that the proposed filter can handle the problem.**

I. Introduction

From mmWave signals sent by a base station (BS), it is possible to obtain highly resolvable channel parameters in time and angular domains [1], [2], enabling accurate mapping of landmarks. Therefore, a variety of radio simultaneous localization and mapping (SLAM) works have been recently developed [1]–[8].

A single type of landmark was considered in [1]–[5]. In [6], the probability hypothesis density (PHD) SLAM filter is developed to track both static and dynamic objects but doesn't keep the track of object types. To track different types of landmarks, the multiple model (MM) PHD filter has been developed [7], applied to mmWave SLAM [8]. It treats moving objects as clutter, under the assumption they are only visible for short intervals. In vehicular mmWave networks, this assumption is violated by moving passive scatterers, leading to incorrect mapping results, depicted in Fig. 1. In particular, a vehicle mmWave receiver can detect scattered signals by neighboring vehicles with dynamics for long periods time [9], called as vehicle scatterer (VS) (i.e., moving passive scatterers) in this work. A VS is detected as a virtual anchor (VA) due to fundamental limit of VS estimation, since the VS velocity cannot be obtained from the mmWave measurements. Thus, these VSs cannot be modeled as clutter anymore.

Mapping in SLAM is closely related to *multi-object tracking* (MOT), where an unknown number of moving objects are detected and tracked with a sensor with the known state. MOT methodologies are developed from belief propagation (BP) [10] and random finite set (RFS) theory [11]. Correspondingly, SLAM methods have been developed using BP-SLAM [1]–[3] and RFS-SLAM [4]–[8]. In BP-SLAM, the landmark state is modeled as a random vector, which requires ad-hoc modifications for addressing the presence of an unknown number of landmarks. Moreover, the correlation between landmark states and sensor state cannot be captured due to density marginalization. In RFS-SLAM, the landmark state is modeled as an RFS, and the RFS density conditioned on the sensor state is propagated. Using the RFS theory, the PHD-SLAM filter that avoids explicit data association is developed, computationally efficient [4]–[8].

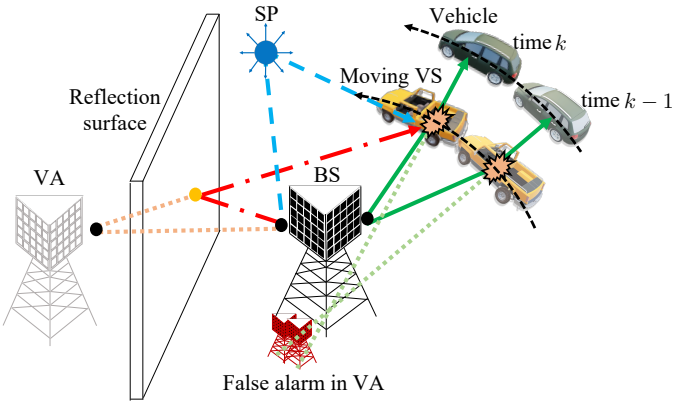

Fig. 1. Channel propagation in mmWave signals, depending on static landmarks (e.g., virtual anchors (VAs) and scatter points (SPs)) and moving vehicle scatterers (VSs). When the VS is regarded as clutter as in [8], false alarms lead to generation of false VAs. Any vehicle that scatters the mmWave signals can be the VS to the neighboring vehicles.

In this paper, we handle the incorrect mapping problem of moving targets by developing an extension of the mmWave radio MM-PHD-SLAM [8] filter. The proposed SLAM filter accounts for passive moving VS and can track the landmarks and moving targets at the same time. Our main contributions are summarized as follows.

- At each vehicle, we propose a local MM-PHD-SLAM filter, treating the PHDs for VS in the context of Bayesian recursion, and modifying the vehicle state correction with the PHD for VS.
- We also develop a new map fusion method to account for the local vehicle posterior in the moving objects map, prior to uploading to the BS.
- At the BS, serving as a fusion center, we introduce a method for asynchronous map fusion, by computing both fusion weights and fused PHDs.
- Via simulations, we show that both local and global approaches must be combined to handle the challenge.

Notation: Variables, random variables, and their realizations are denoted with serif font (e.g., $\mathbf{x}$ for vectors and $\mathbf{X}$ for

matrices), set with calligraphic font (e.g., $\mathcal{X}$). The probability density function and probability mass function are respectively denoted $f(\cdot)$ and $\mathrm{p}(\cdot)$. A Gaussian density with mean $\boldsymbol{\mu}$ and $\boldsymbol{\Sigma}$ is denoted by $\mathcal{N}(\boldsymbol{\mu}, \boldsymbol{\Sigma})$. We denote $d_{(\cdot)}$ by the dimension of random vector $(\cdot)$. The following indexing will be used: vehicle n, target i, time step k, particle p, observed measurement j, and Gaussian mixture (GM) component q.

II. System Model

We consider a downlink mmWave propagation scenario wherein static landmarks that reflect or scatter the radio signals and moving VSs are present.

1) State Definitions: We denote the state of vehicle n at time k by $\mathbf{s}_k^n \in \mathbb{R}^{d_s}$. The targets (static landmarks and moving VSs) are modeled as with PHDs, denoted generically by $D(\mathbf{t}_k, m)$ [11], represented by a GM. Here, $\mathbf{t}_k \in \mathbb{R}^{d_{t(m)}}$ denotes a target state, where the dimension may depend on the target type $m \in \mathcal{M} = \{\mathrm{BS}, \mathrm{VA}, \mathrm{SP}, \mathrm{VS}\}$. For both $\mathbf{s}_k^n$ and $\mathbf{t}_k$, we assume that the first three dimensions correspond to the 3D location.

2) Dynamics: The movement of vehicles and targets is modeled by the transition densities, denoted by $f_{\mathrm{V}}(\mathbf{s}_k^n|\mathbf{s}_{k-1}^n)$ and $f(\mathbf{t}_k|\mathbf{t}_{k-1}, m)$, where targets do not change type. Note that for the BS, the SPs and VAs, there are no dynamics (e.g., $f(\mathbf{t}_k|\mathbf{t}_{k-1}, m = \mathrm{SP}) = \delta(\mathbf{t}_k - \mathbf{t}_{k-1})$).

3) Measurement: Vehicle n can detect signals coming from targets $(\mathbf{t}_k^i, m^i) \in \mathcal{X}$. Signal detection depends on a certain detection probability [2], [3], denoted by $\mathrm{p}_{\mathrm{D},k}(\mathbf{s}_k^n, \mathbf{t}_k^i, m^i) \in [0, 1]$, within the field-of-view (FoV) [12]. Using a channel estimation routine [13] that provides uncertainty estimates, vehicle n obtains an unordered measurement set $\mathcal{Z}_k^n = \{\mathbf{z}_k^{n,1}, ..., \mathbf{z}_k^{n,J}\}$, and $J = |\mathcal{Z}_k^n|$. Measurement includes the time-of-arrival (TOA), angle-of-arrival (AOA) in azimuth and elevation, angle-of-departure (AOD) in azimuth and elevation, of each path, with known measurement covariance matrix. Channel parameters for BS, VAs, and SPs follow the geometric relations in [8, Appendix B]. VSs are also scatterers and thus the relation of VS is the same as that of SP. Note that the geometric relations only hold for either line-of-sight or one-bounce signals [1], [2], [8]. Multi-bounce signals, measurements due to channel estimation error, or briefly visible transient targets (e.g., people) are regarded as clutter, modeled as a Poisson point process. Following [8], [13] non-clutter measurements, say $\mathbf{z}_k^{n,j}$, have an associated likelihood $g(\mathbf{z}_k^{n,j}|\mathbf{s}_k^n, \mathbf{t}_k^i, m_k^i)$, where neither the target index i, nor the target type m_k^i is known.

III. Cooperative MM-PHD-SLAM with VS

To handle the presence of moving VSs, we propose a new MM-PHD-SLAM filter, consisting of local PHD-SLAM and global map fusion. The *local PHD-SLAM filter* is performed at each vehicle, and the vehicle n asynchronously communicates with the BS. Then, the *global map fusion* step is performed at the BS. The diagram for illustrating the proposed algorithm is depicted in Fig. 2.

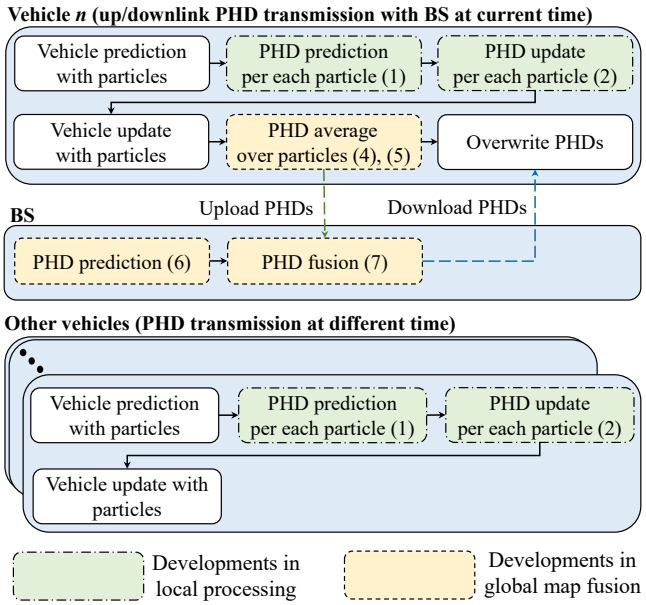

Fig. 2. Diagram for illustrating the proposed MM-PHD-SLAM filter, showing the operation of vehicle n (which is exchanging maps with the BS at time k) on top, the operation of the BS in the middle, and the operation of the other vehicles in the bottom.

A. Local PHD-SLAM

For simplicity, we omit conditioning on past measurements from the PHD and vehicle posterior. The PHD-SLAM filter tracks the vehicle trajectory posterior $f_k(\mathbf{s}_{0:k}^n)$ and computes PHDs for all target types in $\mathcal{M}$. We represent the vehicle posterior with P weighted particles $\mathbf{s}_{0:k}^{n,p}$, i.e., $f_k(\mathbf{s}_{0:k}^n) \approx w_k^{n,p} \sum_p \mathbf{s}_{0:k}^{n,p}$, with $w_k^{n,p} \geq 0$ and $\sum_p w_k^{n,p} = 1$. Given a vehicle state trajectory, $\mathbf{s}_{0:k}^{n,p}$, the posterior PHD $D_{k|k}(\mathbf{t}_k, m|\mathbf{s}_{0:k}^{n,p})$ is a GM with $Q_k(m)$ components.

For each time step k, the local SLAM filter executes a prediction followed by a correction step. The PHD for VS tracks moving targets, while PHDs for the VA and SP track landmarks.

1) Prediction: The vehicle trajectory particle is generated according to the dynamics $\mathbf{s}_k^{n,p} \sim f_{\mathrm{V}}(\mathbf{s}_k^n|\mathbf{s}_{k-1}^{n,p})$ and $w_{k|k-1}^{n,p} = w_{k-1}^{n,p}$. To exploit target dynamics, we include the target transition density $f(\mathbf{t}_k|\mathbf{t}_{k-1}, m)$ in PHD prediction:

$$D_{k|k-1}(\mathbf{t}_k, m|\mathbf{s}_{0:k}^{n,p}) = D_{\mathrm{B},k}(\mathbf{t}_k, m|\mathbf{s}_{0:k}^{n,p}) \tag{1}$$
$$+ P_{\mathrm{S}}(m) \int f(\mathbf{t}_k|\mathbf{t}_{k-1}, m) D_{k-1|k-1}(\mathbf{t}_{k-1}, m|\mathbf{s}_{0:k-1}^{n,p}) \mathrm{d}\mathbf{t}_{k-1},$$

where $P_{\mathrm{S}}(m)$ is the target survival probability, and $D_{\mathrm{B},k}(\mathbf{t}_k, m|\mathbf{s}_{0:k}^{n,p})$ is the PHD for the birth process [5], also modeled by the Poisson point process, to account for generation of new landmarks. For $m = \{\mathrm{VA}, \mathrm{SP}\}$, the PHD for birth is generated by [8, Appendix D-A], using the the cubature Kalman filter (CKF). For VS, we use the same methods as the PHD for SP.

2) Correction: Given the measurement set $\mathcal{Z}_k^n$ and predicted PHDs $D_{k|k-1}(\mathbf{t}_k, m|\mathbf{s}_{0:k}^{n,p})$ for all $m \in \mathcal{M}$ and for each particle, we update the PHDs

$$D_{k|k}(\mathbf{t}_k, m|\mathbf{s}_{0:k}^{n,p}) = (1 - \mathsf{p}_\mathsf{D}(\mathbf{s}_k^{n,p}, \mathbf{t}_k, m))D_{k|k-1}(\mathbf{t}_k, m|\mathbf{s}_{0:k}^{n,p}) + \sum_{\mathbf{z}\in\mathcal{Z}_k^n} \frac{\nu(\mathbf{z}, \mathbf{t}_k, m|\mathbf{s}_{0:k}^{n,p})}{c(\mathbf{z}) + \sum_{m'\in\mathcal{M}} \int \nu(\mathbf{z}, \mathbf{t}_k', m'|\mathbf{s}_{0:k}^{n,p})\mathrm{d}\mathbf{t}_k'}, \quad (2)$$

where $c(\mathbf{z})$ is the clutter intensity and $\nu(\mathbf{z}, \mathbf{t}_k, m|\mathbf{s}_{0:k}^{n,p}) = \mathsf{p}_\mathsf{D}(\mathbf{s}_k^{n,p}, \mathbf{t}_k, m)D_{k|k-1}(\mathbf{t}_k, m|\mathbf{s}_{0:k}^{n,p})g(\mathbf{z}_k|\mathbf{s}_k^{n,p}, \mathbf{t}_k, m)$. The first term in (2) reduces to PHD to account for targets that are no longer in the FoV and thus undetectable. The second term creates a new GM component for each measurement, weighted in the numerator by the detection probability and in the denominator to account for the possibility of the measurement having different origins (clutter or any landmark type in $\mathcal{M}$). Finally, the corrected vehicle weight is

$$w_k^{n,p} \propto w_{k|k-1}^{n,p} \sum_{\mathbf{z}\in\mathcal{Z}_k^n} \{c(\mathbf{z}) + \sum_{m\in\mathcal{M}} \int \nu(\mathbf{z}, \mathbf{t}_k, m|\mathbf{s}_{0:k}^{n,p})\mathrm{d}\mathbf{t}_k\}. \quad (3)$$

B. Global Map Fusion

Periodically, vehicle n performs *average map computation* averaging PHDs over particles for $m \in \mathcal{M}$ and asynchronously communicates with the BS to upload the average PHDs. Note that since a vehicle performing local PHD-SLAM may act as a VS for another vehicle, we should account for the local posterior $f_k(\mathbf{s}_{0:k}^n)$ when computing the average PHD.

At the BS, *map fusion* also accounts for the PHDs for $m \in \mathcal{M}$. The PHD for VS behaves differently from PHDs for VA and SP, and thus we differently design map fusion for VS.

1) Average Map Computation: Vehicle n uploads the averaged PHDs for $m = \{\mathrm{VA}, \mathrm{SP}\}$, expressed as

$$\overline{D}_k^n(\mathbf{t}_k, m) = \sum_{p=1}^{P} w_k^{n,p} D_{k|k}(\mathbf{t}_k, m|\mathbf{s}_{0:k}^{n,p}). \quad (4)$$

For $m = \mathrm{VS}$, the averaged PHD at vehicle n is merged with the local posterior density $f_k(\mathbf{s}_k^n)$, which is obtained from marginalizing $f_k(\mathbf{s}_{0:k}^n)$ (i.e., dropping the first k components from the particles). Then,

$$\overline{D}_k^n(\mathbf{t}_k, \mathrm{VS}) = \mathsf{F}_\mathrm{A}(\widetilde{D}_k^n(\mathbf{t}_k, \mathrm{VS}), f_k(\mathbf{s}_k^n)), \quad (5)$$

where $\widetilde{D}_k^n(\mathbf{t}_k, \mathrm{VS}) = \sum_{p=1}^{P} w_k^{n,p} D_{k|k}(\mathbf{t}_k, \mathrm{VS}|\mathbf{s}_{0:k}^{n,p})$, we consider the marginal posterior $f_k(\mathbf{s}_k^n)$ as a PHD with a single GM component, and $\mathsf{F}_\mathrm{A}(\cdot,\cdot)$ denotes an arithmetic averaging (AA) fusion operator, which will be detailed in Sec. III-C1.

2) Map Fusion: At the BS, there is no measurement, and thus the fused PHD for m is predicted without the birth process

$$\widetilde{D}_{k|k-1}^{\mathrm{BS}}(\mathbf{t}_k, m) = P_\mathrm{S}(m) \int f(\mathbf{t}_k|\mathbf{t}_{k-1}, m)\widetilde{D}_{k-1}^{\mathrm{BS}}(\mathbf{t}_{k-1}, m)\mathrm{d}\mathbf{t}_{k-1}. \quad (6)$$

The fused PHD for m at the BS is computed by fusing the uploaded average PHD from vehicle n (i.e., $\overline{D}_k^n(\mathbf{t}_k, m)$ of (4) or (5)) and the predicted PHD at the BS (i.e., $\widetilde{D}_{k|k-1}^{\mathrm{BS}}(\mathbf{t}_k, m)$ of (6)) as follows:

$$\widetilde{D}_k^{\mathrm{BS}}(\mathbf{t}_k, m) = \mathsf{F}_\mathrm{A}(\widetilde{D}_{k|k-1}^{\mathrm{BS}}(\mathbf{t}_k, m), \overline{D}_k^n(\mathbf{t}_k, m)). \quad (7)$$

Here, the implementation of the AA fusion operator will be detailed in Sec. III-C2. Finally, the fused PHDs $\widetilde{D}_k^{\mathrm{BS}}(\mathbf{t}_k, m)$ for $m \in \mathcal{M}$ are sent to vehicle n, which overwrites its local PHDs as $D_{k|k}(\mathbf{t}_k, m|\mathbf{s}_{0:k}^{n,p}) \leftarrow \widetilde{D}_k^{\mathrm{BS}}(\mathbf{t}_k, m),\ \forall p$.

C. Implementation of AA Fusion

To avoid missed detections in the PHDs, we adopt the AA approach, taking the union of the involved densities. It results in map fusion with minimum information loss [14] by computing the sum of two weighted PHDs with analyzing the proximity between GM components and assigning the fusion weight.

Given 2 PHDs $D_1(\mathbf{t})$ and $D_2(\mathbf{t})$, with Q_1 and Q_2 GM components (i.e., index q_i, weight η_i^q, density $\mathcal{N}^{q_i}(\mathbf{t}) \triangleq \mathcal{N}(\mathbf{t}^{q_i}, \mathbf{T}^{q_i})$, $i \in \{1, 2\}$)

$$\mathsf{F}_\mathrm{A}(D_1(\mathbf{t}), D_2(\mathbf{t})) = \sum_{q_1=1}^{Q_1} \beta_1^{q_1}\eta_1^{q_1}\mathcal{N}_1^{q_1}(\mathbf{t}) + \sum_{q_2=1}^{Q_2} \beta_2^{q_2}\eta_2^{q_2}\mathcal{N}_2^{q_2}(\mathbf{t}),$$

where $\beta_i^{q_i}$ are the fusion weights, which are computed as follows:

(i) computation of an $Q_1 \times Q_2$ proximity matrix $\mathbf{C}$ based on the Mahalanobis distance;
(ii) determining 'matched' components (q_1, q_2) between $D_1(\mathbf{t})$ and $D_2(\mathbf{t})$ if C_{q_1,q_2} is below a threshold; and
(iii) assigning weights $\beta_1^{q_1} = \beta_2^{q_2} = 1/2$ to each matched pair, and assigning weights $\beta_1^{q_1}, \beta_2^{q_2} \in \{1/2, 1\}$ to unmatched components.

Note that $\beta_1^{q_1} + \beta_2^{q_2}$ should be 1 for the matched pairs, not for the unmatched pairs. If the Gaussian q is out of FoV, we determine the Gaussian as false alarm and set $\beta = 1/2$, otherwise, $\beta = 1$.

This general AA fusion is applied to VA and SP in (7). Comparison of AA fusion results between proposed and general methods is depicted in Fig. 3.

1) VS Average Map (5)*:* First, we compress $\widetilde{D}_k^n(\mathbf{t}_k, \mathrm{VS}) = \sum_p w_k^{n,p} D_{k|k}(\mathbf{t}_k, \mathrm{VS}|\mathbf{s}_{0:k}^{n,p})$ by standard pruning and merging (PM) [4, Table IV] to obtain a GM with few components, say $\widetilde{D}_k^n(\mathbf{t}_k, \mathrm{VS}) \approx \sum_{q=1}^{Q} \eta^q\mathcal{N}^q$. We consider $f_k(\mathbf{s}_k^n)$ as a Gaussian distribution of the form $f_k(\mathbf{s}_k^n) \approx \mathcal{N}(\mathbf{t}_{k|k}^n, \mathbf{T}_{k|k}^n)$. Second, we generate a binary proximity vector $\mathbf{c} \in \{0, 1\}^Q$, with element $c^q = 1$ if and only if

$$d_\mathrm{M}^{1:3}(\mathcal{N}^q(\mathbf{t}), \mathcal{N}^n(\mathbf{t})) < T_\mathrm{M}^L,$$

where T_M^L is the threshold, and $d_\mathrm{M}^{1:3}(\cdot,\cdot)$ denotes a maximum symmetric Mahalanobis (MSM) distance considering the first 3 components of the vehicle or VS state, defined as

$$d_\mathrm{M}^{1:3}(\mathcal{N}^1(\mathbf{t}), \mathcal{N}^2(\mathbf{t})) = \max(\boldsymbol{\Delta}^\top\boldsymbol{\Sigma}_1^{-1}\boldsymbol{\Delta}, \boldsymbol{\Delta}^\top\boldsymbol{\Sigma}_2^{-1}\boldsymbol{\Delta})$$

with $\boldsymbol{\mu}_i = [\mathbf{t}_i]_{1:3}$, $\boldsymbol{\Sigma}_i = [\mathbf{T}_i]_{1:3,1:3}$, and $\boldsymbol{\Delta} = \boldsymbol{\mu}_1 - \boldsymbol{\mu}_2$. Finally, we set the fusion weights as $\beta_1^q = 0$ when $c^q = 1$

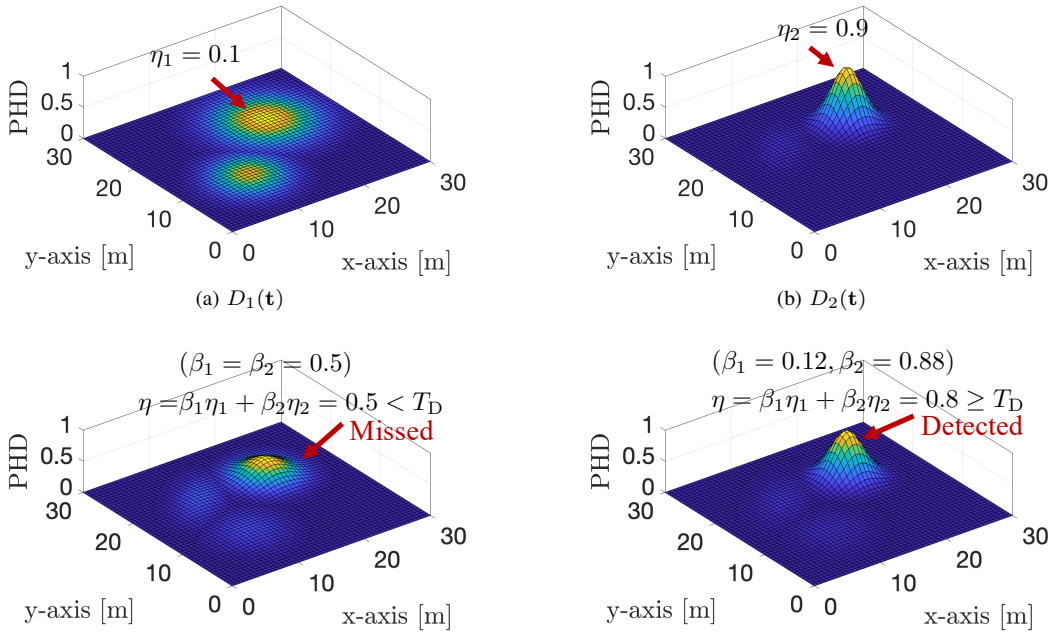

(a) $D_1(\mathbf{t})$ (b) $D_2(\mathbf{t})$

(c) General $\mathsf{F}_{\mathrm{A}}(D_1(\mathbf{t}), D_2(\mathbf{t}))$ [8] (d) Proposed $\mathsf{F}_{\mathrm{A}}(D_1(\mathbf{t}), D_2(\mathbf{t}))$

Fig. 3. Comparison of AA fusion results between proposed and general methods. Two PHDs (a) $D_1(\mathbf{t})$ and (b) $D_2(\mathbf{t})$ are fused. The VS is missed ($\eta < T_{\mathrm{D}}$) by (c) general AA fusion [8] while it can be detected ($\eta \geq T_{\mathrm{D}}$) by (d) proposed AA fusion. Here, T_{D} is the threshold.

and $\beta_1^q = 1$ otherwise, and $\beta_2^q = 1$. Here, $c^q = 1$ indicates that vehicle posterior is matched to Gaussian q in PHD for VS. This ensures that matched GM components in the PHD for VS are removed and replaced with a weighted vehicle posterior.

2) VS Map Fusion (7)*:* We consider $\overline{D}_k^n(\mathbf{t}_k, \mathrm{VS})$ to be a GM with Q^{UE} components and $\widetilde{D}_{k|k-1}^{\mathrm{BS}}(\mathbf{t}_k, \mathrm{VS})$ a GM with Q^{BS} components. We generate a matrix $\mathbf{C} \in \{0,1\}^{Q^{\mathrm{BS}} \times Q^{\mathrm{UE}}}$, indicating the proximity between two targets, with $C_{q_1,q_2} = 1$ if and only if the following two conditions are satisfied:

$$d_{\mathrm{M}}^{1:3}(\mathcal{N}^{q_1}(\mathbf{t}), \mathcal{N}^{q_1}(\mathbf{t})) < T_{\mathrm{M}}^L, \quad d_{\mathrm{M}}^{4:6}(\mathcal{N}^{q_1}(\mathbf{t}), \mathcal{N}^{q_1}(\mathbf{t})) < T_{\mathrm{M}}^V,$$

where T_{M}^V is a threshold and $d_{\mathrm{M}}^{4:6}$ computes the MSM distance on the velocity, assumed to correspond to dimension 4 through 6 in the VS state. The fusion weights are finally assigned as follows:

- *Matched Targets* (i.e., $C_{q_1,q_2} = 1$): Targets with means $\mathbf{t}^{q_1}$ and $\mathbf{t}^{q_2}$ are matched so that two VS densities need to be merged. To weigh the matched densities according to their covariance, the Gaussian uncertainty is determined by $\rho = \dim(\mathbf{t})/\mathrm{trace}(\mathbf{T})$. Then, we compute the weights as

$$\beta_1^{q_1} = \rho^{q_1}/(\rho^{q_1} + \rho^{q_2}), \qquad \beta_2^{q_2} = \rho^{q_2}/(\rho^{q_1} + \rho^{q_2}) \quad (8)$$

- *Unmatched Targets* (i.e., $\sum_{q_1} C_{q_1,q_2} = 0$ or $\sum_{q_2} C_{q_1,q_2} = 0$): Targets with means $\mathbf{t}^{q_1}$ and $\mathbf{t}^{q_2}$ are unmatched. If $\sum_{q_1} C_{q_1,q_2} = 0$, then the Gaussian q_2 is not associated with any Gaussian q_1, indicating that Gaussian q_2 could be a newly detected target or false alarm. To avoid the risk of missed detection, we set $\beta_2^{q_2} = 1$. If $\sum_{q_2} C_{q_1,q_2} = 0$, then Gaussian q_1 is not associated with any Gaussian q_2, indicating that Gaussian q_1 could be the previously detected target or previous false alarm. Here, we can make a decision based on the accumulated FoV. If $\mathbf{t}^{q_1}$ was not in the FoV of the vehicle, then Gaussian q_1 is decided as the previously detected target by other vehicles and thus we set $\beta_1^{q_1} = 1$ for keeping Gaussian q_1 as a previously detected target that was outside the FoV of the vehicle. If $\mathbf{t}^{q_1}$ was in the FoV of the vehicle, then Gaussian q_1 is decided as a previous false alarm, since it should have been detected by the vehicle if it was a real target. We set $0 < \beta_1^{q_1} < 1$ (e.g., 0.25) for reducing the weight of the Gaussian q_1 density generated by possible previous false alarm, while simultaneously preventing missed detections.

IV. Simulation Results and Discussions

A. Simulation Setup

To demonstrate the developed PHD-SLAM filter to handle VSs, we consider a scenario that VS measurements are added into mmWave radio propagation environment as shown in Fig. 4. We consider two vehicles which move parallel on the circular road, and a single BS, four VAs, and four SPs are located in the environment. The same values in [8, Sec. VI-A] are adopted for the parameters as follows: process noise $\mathbf{q}_k$ of the vehicle dynamics in polar coordinates; time interval Δ, measurement noise covariance $\mathbf{R}$; BS location $\mathbf{x}_{\mathrm{BS}}$, VA locations $\mathbf{x}_{\mathrm{VA},1}$, $\mathbf{x}_{\mathrm{VA},2}$, $\mathbf{x}_{\mathrm{VA},3}$, $\mathbf{x}_{\mathrm{VA},4}$; threshold for PM steps (for the reduction of Gaussian components and the weighted sum

of Gaussians); threshold for target detection T_{VA}, $T_{\text{VS}} = T_{\text{SP}}$; birth weight; Poisson mean for clutter measurement; landmark visibility and FoV range $r_{\text{SP}} = r_{\text{VS}} = 50$ m. In the birth process of (1), correction leads to overly concentrated covariance estimates [15] due to the nonlinear measurement model, and the fact that the VS velocity and turn-rate in the PHD for VS birth cannot be observed. To address this, we adopt the dithering methods, mitigating approximation error for target estimates in the CKF [16].

For dynamics of vehicle states, we respectively adopt [8, eq. (25)] in polar coordinates and [17, Sec. V-B] in Cartesian coordinates, rendering the VS state identifiable over time. We set the process noise standard deviations of the dynamics in Cartesian coordinates to $[1, 1, 0.1, 3, 3, 0.1, 0.05]^\top$, with units m, m, m, m/s, m/s, m/s, rad/s. For generating VS velocity $\mathbf{v}$ and turn-rate ξ in $D_{\text{B},k}(\mathbf{t}_k|\mathbf{s}_{0:k}^{n,p})$ of (1), we set the VS velocity covariance $\mathbf{V} = \text{diag}([100, 100, 0.09])$ and turn-rate standard deviation $\sigma_\xi = \pi/2$. The velocity and turn-rate are respectively sampled from $\mathbf{v} \sim \mathcal{N}(\mathbf{0}, \mathbf{V})$ and $\xi \sim \mathcal{U}(0, 2\pi]$. In VS prediction, $\mathbf{T}_d = \text{diag}([9, 9, 0.09, 5, 5, 0.09, 0.18])$ is added into each covariance of VS Gaussians during (1). The vehicle states are initialized as $\mathbf{s}_0^1 = [70.73, 0, 0, \pi/2, 22.22, \pi/10, 300]^\top$ and $\mathbf{s}_0^2 = [60.73, 0, 0, \pi/2, 19.08, \pi/10, 300]^\top$, with units m, m, m, rad, m/s, rad/s, and m. The initial prior of the vehicle state is sampled from $\mathcal{N}(\mathbf{s}_0^n, \mathbf{S}_0^n)$, where $\mathbf{S}_0^n = \text{diag}(0.3^2, 0.3^2, 0, 0.1^4, 0, 0, 0.3^2)$. The longitudinal velocity ζ_k^n and turn-rate ξ_k^n of the vehicle n are assumed to be known since the knowledge of inertial sensor of board is available. Four SPs are located at $[\pm 55, \pm 55, z_{\text{SP}}]^{\text{T}}$ m, where $z_{\text{SP}} \sim \mathcal{U}(0, 40)$. We set $p_{\text{D}} = 0.95$ within the FoV and $P(m) = 0.99$.

After the PHD fusion, the PM step in [4, Table IV] is used in averaging PHDs (4). In the PM steps of averaging PHDs and PHD fusion, the pruning threshold is set to 0.1, preventing the false Gaussian with large covariance from diluting the true Gaussian with small covariance. Both thresholds M_{M}^L and M_{M}^V are set to 20. In asynchronous map fusion, vehicles communicate with the BS every 2 time steps, with vehicle 1 and vehicle 2 respectively starting at time 5 and 6. For representing each vehicle state, $P = 300$ particles are used, and results are averaged over 10 Monte Carlo runs. To evaluate the mapping accuracy, the average of the generalized optimal subpattern assignment (GOSPA) distance is utilized.

B. Results and Discussion

1) Mapping: Fig. 5 shows the mapping accuracy of the proposed filter, evaluated by averaging GOSPA distances. The VS measurement cannot be handled by the MM-PHD-SLAM filter [8] with the additional PHD for VS and dynamics. Thus, false detection appears in the PHD for VA as shown in Fig. 5b, and inevitably the VS target is missed as shown in Fig. 5a. The proposed MM-PHD-SLAM filter without development in (7) can improve the SLAM accuracy since the VS measurement is handled since the VS velocity can be obtained with the self-vehicle posterior density in (5) of the global map fusion step. We confirm that the proposed MM-PHD-SLAM filter (i.e., with both (5) and (7)) handles the challenge (false alarms in the PHD for VA and missed detections in the PHD for VS, due to VS measurements) by virtue of the proposed fused PHD.

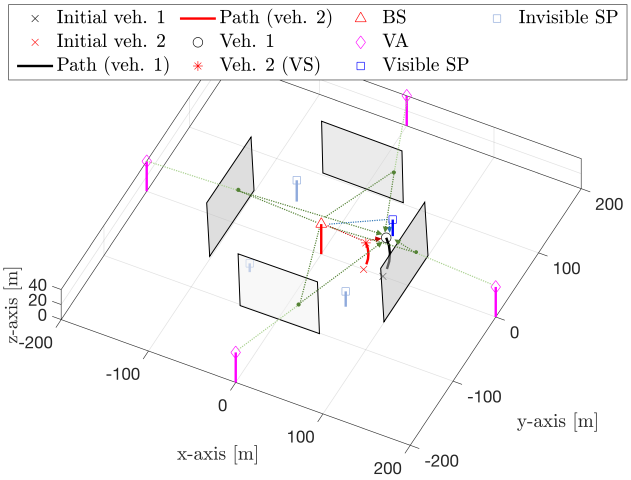

Fig. 4. Two vehicles are moving. When the vehicle 1 is the active vehicle, the vehicle 2 is passive vehicle which acts as the VS. Here, the propagation environment consists of 1 BS, 4 VAs, 4 SPs, and 1 VS (i.e., vehicle 2).

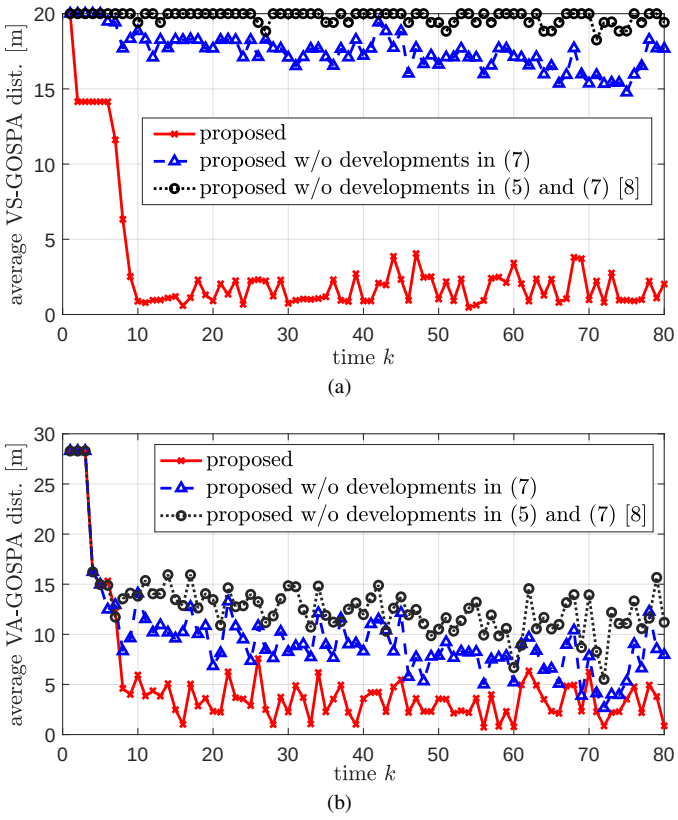

Fig. 5. Mapping performance: Average GOSPA of (a) VS and (b) VA.

2) Localization: Fig. 6 shows the accuracy of the vehicle state estimates, evaluated by the root mean square error (RMSE) for the location (similar behavior was observed for the clock bias and heading). For the filter from [8] and the

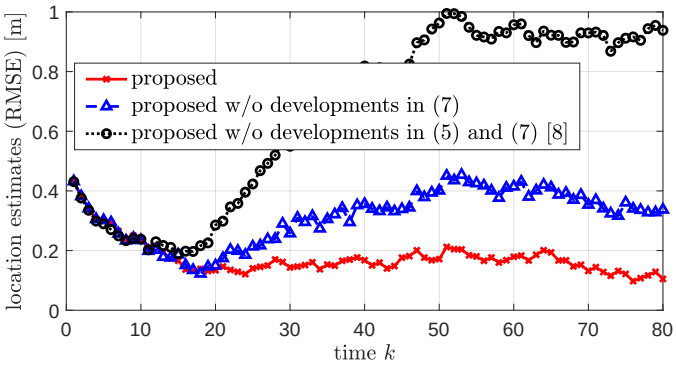

Fig. 6. Localization performance: Average error of vehicle state estimates in terms of location RMSE.

proposed MM-PHD-SLAM filter, we observe similar trends as in mapping, due to the fact that vehicle and map are correlated at every time step. The RMSEs are similar at first. However, after starting map fusion at time 5, and after a few time steps, the fused map is becoming informative, then the RMSEs diverge.

V. Conclusions

To handle moving VSs in SLAM, we have proposed the cooperative mmWave radio PHD-SLAM filter. We demonstrated that the standard radio MM-PHD-SLAM filter [8] fails, due to the false targets raised by the VSs. The posterior density of the local vehicle is included in the PHD for VS by a novel fusion rule, enabling to avoid missed detection of the VS by preventing covariance from increasing over time. We confirmed that the proposed filter can track both moving VSs and static landmarks (VAs and SPs), while simultaneously localizing the vehicles.

Acknowledgments

This work was supported in part by the MSIP, Korea, under the ITRC support program (IITP-2022-2017-0-01637), and by the Wallenberg AI, Autonomous Systems and Software Program (WASP) funded by the Knut and Alice Wallenberg Foundation, the Vinnova 5GPOS project under grant 2019-03085.

References

[1] E. Leitinger, F. Meyer, F. Hlawatsch, K. Witrisal, F. Tufvesson, and M. Z. Win, "A belief propagation algorithm for multipath-based SLAM," *IEEE Trans. Wireless Commun.*, vol. 18, no. 12, pp. 5613–5629, Dec. 2019.

[2] E. Leitinger, S. Grebien, and K. Witrisal, "Multipath-based SLAM exploiting AoA and amplitude information," in *IEEE Int. Conf. Commun. Workshops (ICC Workshops)*, Shanghai, China, May 2019, pp. 1–7.

[3] G. Soldi, F. Meyer, P. Braca, and F. Hlawatsch, "Self-tuning algorithms for multisensor-multitarget tracking using belief propagation," *IEEE Trans. Signal Process.*, vol. 67, no. 15, pp. 3922–3937, Aug. 2019.

[4] J. Mullane, B.-N. Vo, M. D. Adams, and B.-T. Vo, "A random-finite-set approach to Bayesian SLAM," *IEEE Trans. Robot.*, vol. 27, no. 2, pp. 268–282, Apr. 2011.

[5] L. Gao, G. Battistelli, and L. Chisci, "Random-finite-set-based distributed multirobot SLAM," *IEEE Trans. Robot.*, vol. 36, no. 6, pp. 1758–1777, 2020.

[6] C. S. Lee, D. E. Clark, and J. Salvi, "SLAM with dynamic targets via single-cluster PHD filtering," *IEEE J. Sel. Topics Signal Process.*, vol. 7, no. 3, pp. 543–552, 2013.

[7] K. Y. Leung, F. Inostroza, and M. Adams, "Multifeature-based importance weighting for the PHD SLAM filter," *IEEE Trans. Aerosp. and Electron. Syst.*, vol. 52, no. 6, pp. 2697–2714, 2016.

[8] H. Kim, K. Granström, L. Gao, G. Battistelli, S. Kim, and H. Wymeersch, "5G mmWave cooperative positioning and mapping using multi-model PHD," *IEEE Trans. Wireless Commun.*, vol. 19, no. 6, pp. 3782–3795, Mar. 2020.

[9] C. U. Bas, R. Wang, S. Sangodoyin, S. Hur, K. Whang, J. Park, J. Zhang, and A. F. Molisch, "Dynamic double directional propagation channel measurements at 28 GHz," *arXiv preprint arXiv:1711.00169*, 2017.

[10] F. Meyer, T. Kropfreiter, J. L. Williams, R. Lau, F. Hlawatsch, P. Braca, and M. Z. Win, "Message passing algorithms for scalable multitarget tracking," *Proc. IEEE*, vol. 106, no. 2, pp. 221–259, 2018.

[11] R. Mahler, *Statistical Multisource-Multitarget Information Fusion*. Norwood, MA, USA: Artech House, 2007.

[12] H. Wymeersch and G. Seco-Granados, "Adaptive detection probability for mmWave 5G SLAM," in *6G Wireless Summit (6G SUMMIT)*, 2020.

[13] Y. Ge, F. Wen, H. Kim, M. Zhu, F. Jiang, S. Kim, L. Svensson, and H. Wymeersch, "5G SLAM using the clustering and assignment approach with diffuse multipath," *Sensors*, vol. 20, no. 16, 2020.

[14] L. Gao, G. Battistelli, and L. Chisci, "Multiobject fusion with minimum information loss," *IEEE Signal Process. Lett.*, vol. 27, pp. 201–205, Jan. 2020.

[15] S. Huang and G. Dissanayake, "Convergence and consistency analysis for extended Kalman filter based SLAM," *IEEE Trans. Robot.*, vol. 23, no. 5, pp. 1036–1049, Oct. 2007.

[16] F. Gustafsson and G. Hendeby, "On nonlinear transformations of stochastic variables and its application to nonlinear filtering," in *Proc. IEEE Int. Conf. Acoust. Speech Signal Process. (ICASSP'08)*, 2008, pp. 3617–3620.

[17] X. Rong-Li and V. Jilkov, "Survey of maneuvering target tracking: Part I. Dynamic models," *IEEE Trans. Aerosp. Electron. Syst.*, vol. 39, no. 4, pp. 1333–1364, Oct. 2003.